Mineral chemistry of Turkana basalts and implications for basin development

Karla Knudson, Louise Miltich, Nick Swanson-Hysell

Department of Geology, Carleton College, Northfield, MN 55057

Abstract

Geochemistry of plagioclase, pyroxene, and ilmenite phenocrysts from Turkana basin basalts were analyzed in order to determine if they resulted from a common magma chamber, as suggested by previous studies by Haileab et al. (2004). Electron microprobe results indicated chemically-similar phenocrysts throughout all samples. SiO_2 content for the Gombe basalts was between 48 and 51 wt%, and each of the oxides Al_2O_3, Fe_2O_3, TiO_2, MgO, MnO, CaO, Na_2O, K_2O, P_2O_5 showed a range of about 1 wt%. Normalized composition of most plagioclase phenocrysts was 60 to 70 wt% anorthite, with some samples exhibiting weak zoning, becoming more anorthite rich toward the edge. Most ilmenite grains had normalized percentage values for Fe_2O_3, TiO_2, and FeO each around 30-35%, regardless of their location at the core or the rim of the grain. Pyroxene phenocryst chemistry showed compositional zoning and are mostly diopside-hedenbergite with little to no jadite component. Geothermometer equations based on pyroxene chemistry were used to calculate crystallization temperatures between 1093°C and 1182°C. Thermobarometer equations yielded an estimated upper limit of pressure at 5.37 kBar, and suggest that the parent magma chamber was located less than 18 km below the earth's surface.

Introduction

Today, the Turkana basin is filled with basalt from Pleiocene tectonic activity. The period of volcanic activity has been constrained to a short time interval, 3.9-4.18 Ma (Haileab et al., 2004). The basalts that were produced throughout the basin have been correlated petrographically and chemically and grouped together as the Gombe basalts (Haileab et al., 2004). In order to further correlate these basalts and to determine if they

resulted from a common magma chamber we studied the geochemistry of individual phenocrysts.

Using an electron microprobe, we examined the composition of pyroxene, plagioclase, and ilmenite crystals in basalt samples from throughout the basin. We found the phenocrysts from each sample to be chemically similar, further supporting the findings from whole rock geochemistry work, which categorize these basalts as stemming from a similar magma source (Haileab et al., 2004). Geothermobarometry techniques were used to characterize the parent magma chamber and cooling conditions of these basalts. We were able to determine that these basalts formed at low pressures (<5 kBar); however actual pressures could not be resolved using this technique. Using pyroxene core chemistry we determined initial crystallization temperatures between 1127° C and 1182° C.

In this study, using the phenocryst geochemistry and the derived temperatures and pressures of the crystallizing magma, we have generated a model for basin development in the Turkana depression. We propose that thermal erosion and extension resulted in pooling of magma at the base of the crust. This magma erupted, creating a single flood basalt that covered the floor of the basin, resulting in the nearly homogenous basalts found in the Turkana region today.

Geological Setting

The Turkana basin is the locus of a period of regional tectonic rifting activity that began shortly before 4 Ma in northeastern Africa (Haileab et al., 2004). Regional extension, sediment deposition, and basaltic volcanism occupied a relatively narrow band

between 6°45' N and 2°45'N and extended from southern Ethiopia through northern Kenya (Fig. 1). Today, the northern portion of the basin accommodates the Omo river while the southern part is occupied by Lake Turkana. The depression is bounded on either side by normal faulting that has created the plateaus east of Lake Turkana and a series of half grabens in the rifting region (Fig. 1).

The region is composed of Precambrian basement rocks that are overlain by Paleogene sediments and volcanics followed by sediments interlayered with thin flood basalt flow resulting from Pliocene and Pleistocene rifting. The Pliocene and Pleistocene strata that outcrop in the Omo region are referred to as the Mursi Basalts (including basalts in the Mursi, Nkalabong, Usno, Shungura, Nachukui and Koobi Fora Formations) (Haileab et al., 2004) while those that outcrop on or near the Sergei and Gombe plateaus east of Lake Turkana are grouped as the Gombe Basalts (Haileab et al., 2004). Seismic reflection data indicates that the basalt layer extends across the entire area now covered by Lake Turkana and in some areas in the North where it is covered by Omo River sediments (Haileab et al., 2004). The basalts throughout the region were emplaced within a very short time span (3.99-4.18 Ma) and through whole rock geochemistry have been reconciled to a single group allowing them to be referred to as the Gombe Group basalts (Haileab et al., 2004).

Petrography

Whole rock geochemical analysis has shown the Turkana basalts to be remarkably homogeneous (Haileab et al., 2004). Samples from across the region are medium grained, compositionally borderline between alkaline and tholeiitic and chemically

distinct from surrounding volcanics (Haileab et al., 2004). They are composed mostly of plagioclase (50%), clinopyroxene (20%), glass (20%) and titanium-rich ilmenite and rarely olivine. The texture is aphyric with glass and small (1mm) subhedral phenocrysts of interlocking plagioclase forming the matrix into which smaller (.5mm) euhedral crystals of clinopyroxene have grown. Ilmenite occurs as thin, branching, dendritic crystals. Alteration is uncommon except where some of the glass has been altered to chlorite.

Chemical composition is similar across samples with SiO_2 content for the Gombe basalts lying between 48 and 51wt%, and each of the oxides Al_2O_3, Fe_2O_3, TiO_2, MgO, MnO, CaO, Na_2O, K_2O, P_2O_5 showing a range of only about 1 wt%. MgO, K_2O, P_2O_5, Na_2O, TiO_2 and MnO each compose a small weight percent of total composition (<5 wt%), while CaO, Al_2O_3, and Fe_2O_3 each compose between 8 and 15 wt% of the total. These basalts are higher in TiO_2 and SiO_2 than nearby volcanics and comparatively depleted in MgO, CaO and Fe (Haileab et al., 2004).

Methods

Thin sections used in this study were provided by Professor Bereket Haileab and contained basalts which were collected from the Turkana depression. All chemical analyses were done in March 2004, at the University of Minnesota's Electron Microprobe Laboratory, using its JEOL 8900 "Super Probe" Electron Probe Microanalyzer. Before probing, thin sections were prepared using a JEOL JEE-400 Vacuum Evaporator to coat them with a thin layer of carbon. The microprobe was calibrated using augite-032, labrodorite-028 and illmenite 021 standards. During probing, the accelerating voltage was

15 kV, and the beam diameter was 5 microns at the sample surface although the interaction volume was probably more like 6 or 7 microns in diameter. Thin sections were probed both in lines traversing from the core to rim of grains, as well as in single points at a core or rim. Pyroxene, plagioclase, and ilmenite were selected and were identified by electron backscatter imaging. Microprobe data was reported as weight percent for each chemical group: SiO_2, TiO_2, Na_2O, Cr_2O_3, FeO, Al_2O_3, CaO, MgO, and MnO. After discarding samples which had chemical group totals that were not approximately 100%, we normalized the chemistry for each mineral to find its end-member composition.

This study attempted to use clinopyroxene phenocryst chemistry to estimate temperature and pressure using a geothermobarometer calibrated by Purtika et al. (1996). This geothermobarmeter was calibrated for pressures ranging between 8 and 30 kBar. Because we did not probe the glass, whole rock chemistry was used as a proxy for liquid composition. Equation (i) uses the jadeite-diopside/hedenbergite exchange equilibrium and works as a geothermometer. Equation (ii) is particularly sensitive to jadeite formation and uses the temperature calculated in (i) to calculate pressures (in kBar).

$$\text{(i)}\quad \frac{10^4}{T} = 6.73 - 0.26 * \ln\left[\frac{Jd^{px} * Ca^{liq} * Fm^{liq}}{DiHd^{px} * Na^{liq} * Al^{liq}}\right] - 0.86 * \ln\left[\frac{Mg^{liq}}{Mg^{liq} + Fe^{liq}}\right] + 0.52 * \ln\left[Ca^{liq}\right]$$

$$\text{(ii)}\quad P = -54.3 + 299 * \frac{T}{10^4} + 36.4 * \frac{T}{10^4} \ln\left[\frac{Jd^{px}}{[Si^{liq}]^2 * Na^{liq} * Al^{liq}}\right] + 367 * [Na^{liq} * Al^{liq}]$$

Mineral Chemistry:

Plagioclase

Plagioclase phenocrysts are abundant in these basalts and occur as euhedral to subhedral crystals sometimes forming interlocking groups with individual phenocrysts varying in size from less than .25mm to .5mm (Fig. 2). The size and pattern of crystal growth varied only slightly between samples, with WS-8 and K83-1694 containing the smallest grains with diameters only slightly larger than 100 μm. Phenocrysts in samples from the Nkalabong region were significantly more interlocked and subhedral than elsewhere. Plagioclase crystals rarely showed visually observable compositional zoning and showed no apparent alteration.

Plagioclase composition was relatively uniform across samples (Fig. 3). Most samples plotted with normalized weight percentages in the 60-70 wt% anorthite range and occasionally showed weak zoning, becoming more anorthite rich toward the rim (Tables 1-6 and Fig. 4). Probing of phenocrysts in sample number WS-8 yielded a maximum anorthite content of 78.83 wt% and a minimum of 57.4 wt%. Core values ranged from 57.4 wt% to 67.79 wt% while rim values ranged from 58.13 wt% to 78.83 wt%. Results from K90-4661 show a similar trend with core values between 63.43 wt% and 66.98 wt% anorthite and rim values between 66.84 wt% and 70.21wt% anorthite. Transects across the smaller grains in WS-8 were less predictable but one good sample gave a core measurement of 52.9 wt% anorthite and a rim value of 64.15 wt%. K00-6133 values were tightly clustered with cores ranging from 61.6 wt% and 66.49 wt% anorthite and rims between 62.56 wt% and 65.26 wt% anorthite. NK-51 yielded one very long transect displaying variable zoning from 65.43 wt% to 59.79 wt% anorthite, two

shorter transects gave ranges from 60.01 wt% to 67.03 wt% and from 65.81 wt% to 66.01 wt% anorthite. Sample number NK-45 followed the trend giving core values in the range 66.84 wt% to 67.09 wt% and rim values from 67.02 wt% to 67.61 wt% anorthite.

Ilmenite

The Fe-Ti oxide ilmenite occurred in tabular, bladed phenocrysts within the Turkana basalt thin sections. Although large enough to be considered phenocrysts, ilmenite grains were smaller in size compared to the plagioclase and pyroxene grains (Fig. 5). Ilmenite crystals did not visually show compositional zoning and had distinct grain boundaries that displayed no apparent chemical alteration.

The compositions of the grains were fairly consistent throughout the samples, regardless of their location at the core or the rim of the grain (Table 7). Most samples (K83-1694, K90-4661, WS-8, and K00-6133) had normalized percentage values for Fe_2O_3, TiO_2, and FeO each around 30-35%. The nearly equivalent end-member compositions caused the ilmenite grains to be plotted near the center of the phase diagram (Fig. 5). As shown in Table X, sample NK-45, however, had slightly lower titanium composition (normalized value of 11.46%), and higher levels of Fe_2O_3 (46.57%) and FeO (41.96 %), which caused its points to plot further away from TiO_2 (Fig. 5). No valuable results were obtained from sample NK-51, since the ilmenite grains that were probed within this sample were too small to provide accurate data, especially when points were probed in a line.

Pyroxene

The clinopyroxenes in the basalts occur as sparse small euhedral phenocrysts. The pyroxenes were all very chemically similar. As can be seen in (Fig. 6) the percentages of silica and magnesium are near equal for all samples. This chemical similarity can be seen in Tables 8-13. The pyroxenes are predominantly diopside-hedenbergite and contain little to no jadeite. The phenocrysts were compositional zoned in that Mg content decreased towards the rim. Table 14 shows representative pyroxene chemistry in each of the basalts for core and rim points. Particularly of note in this table is that for all samples the Mg/(Mg+Fe) ratio is greater in the core than at the rim. Fig. 7 shows a transect across a grain, with Mg content decreasing in a linear fashion towards the rim.

Geothermobarometry

The geothermometer produced results for the core of K-90-4661, 1127 ˚C, the core of WS-8, 1182 ˚C, and the rim of WS-8, 1090˚C. The thermobarometer was used to calculate a pressure of 5.37 kBar for WS-8 core (~ 18 km depth). Other pressures are less than 5 kBar and could not be calculated.

Discussion

Phenocryst analyses reinforce the similarities between samples observed in whole rock geochemical analysis and allow Gombe basalts to be attributed to a single magma chamber at a depth of less than 18 km. The chemical similarities of pyroxene, plagioclase and ilmenite phenocrysts across samples indicate a common magmatic origin.

The decreased Mg content at the rims relative to the core of the pyroxene phenocryst is an indication that as the phenocryst was crystallizing it moved to lower pressures in the melt. There was upward movement in the magma chamber before the melt erupted. The linear fashion in which this zoning occurs indicates that this movement was constant. The temperature data calculated for WS-8 confirms this as the temperature calculated for the core is higher than the temperature calculated for the rim.

Pressure and temperature calculations based on pyroxene chemistry place the magma chamber at relatively low pressure. Pressure and temperature calculations were limited, howeverm by the thermobarometry technique that we used, which was calibrated for higher temperatures and pressures than were experienced during the crystallization of the phenocrysts in the Gombe basalts. The geothermobarometer used in this study was calibrated between 8 and 30 kBar. Both the barometer and the thermometer rely on aluminum filling up the tetrahedral sites and starting to fill octahedral sites, thereby creating a jadiete component. They are both particularly sensitive to a jadeite component and sufficient aluminum in the system. Because of the low aluminum content in the pyroxenes, the jadeite component was often zero and pressures could not be calculated. Thus, temperatures and pressures in a low pressure system, like the magma chamber the Gombe basalt where in during phenocryst development, can not be accurately determined, if they can be determined at all, using the methods of Putirka et al. (1996). What we can say is that the one pressure we were able to calculate, 5.37 kBar for the core of WS-8, is the upper limit in terms of pressure. The magma chamber that produced these basalts was at 5 kBar of pressure or less and temperatures were in the range of 1100˚C.

We propose a model of plume generated thermal erosion at the base of the lithosphere accompanied by crustal extension. This process resulted in thinning, subsidence and sedimentation into the newly formed basin. Possibly exploiting a suture zone in the Precambrian basement (Burke et al., 2003), magma ponded at the base of the thinned crust and eventually erupted over the layer of early sediments as a thin (<100 m) basalt flow. Rifting activity continued resulting in normal faulting and subsequent layers of sediments and volcanoclastics covering the Gombe basalts.

Conclusion

Chemical analysis of pyroxene, plagioclase and ilmenite phenocrysts from Turkana basin basalts confirms that these basalts share a common origin. Geothermobarometry calculations indicate a relatively low crystallization pressure and moderate temperatures.

Acknowledgments

We would like to thank Professor Bereket Haileab for providing us with our thin sections of Turkana basalts and for his instruction in our research and in writing this paper. Thanks also to Ellery Frahm at the University of Minnesota Electron Microprobe Laboratory for introducing us to the equipment and helping us to collect data and to Professor Cameron Davidson for his guidance in interpreting the structural geology aspect of this project.

References

Burke K., Lewis D. A., Webb S. J. 2003. New way to map old sutures using deformed alkaline rocks and carbonatites. Geology, V. 31, p. 391–394.

Haileab, Bereket, Francis H. Brown, Ian McDougall, Patrick N. Gathogo, 2003. Gombe Group basalts and initiation of Pliocene deposition in the Turkana depression, northern Kenya and southern Ethiopia. *Geological Magazine*, V. 141, 41-53.

Putirka K., Johnson M., Kinzler R, Longhi J, Walker D. 1996. Thermobarometry of mafic igneous rocks based on clinopyroxene-liquid equilibria, 0-30 kbar. *Contributions to Mineralalogy and Petrology* 123, 92-108.

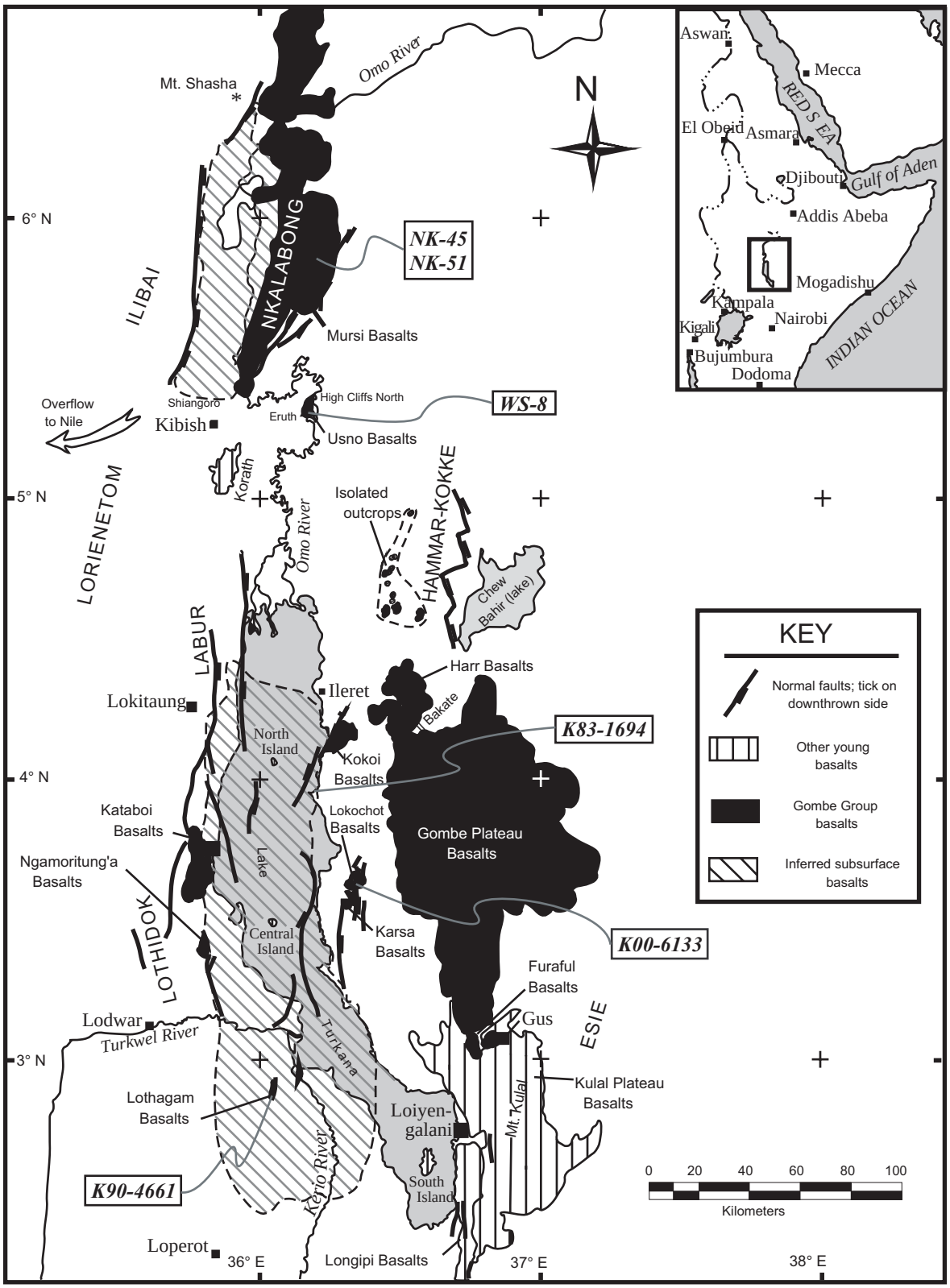

Figure 1: Location map for the basalts analyzed in this study. Map modified from (Haileab et al 2004).

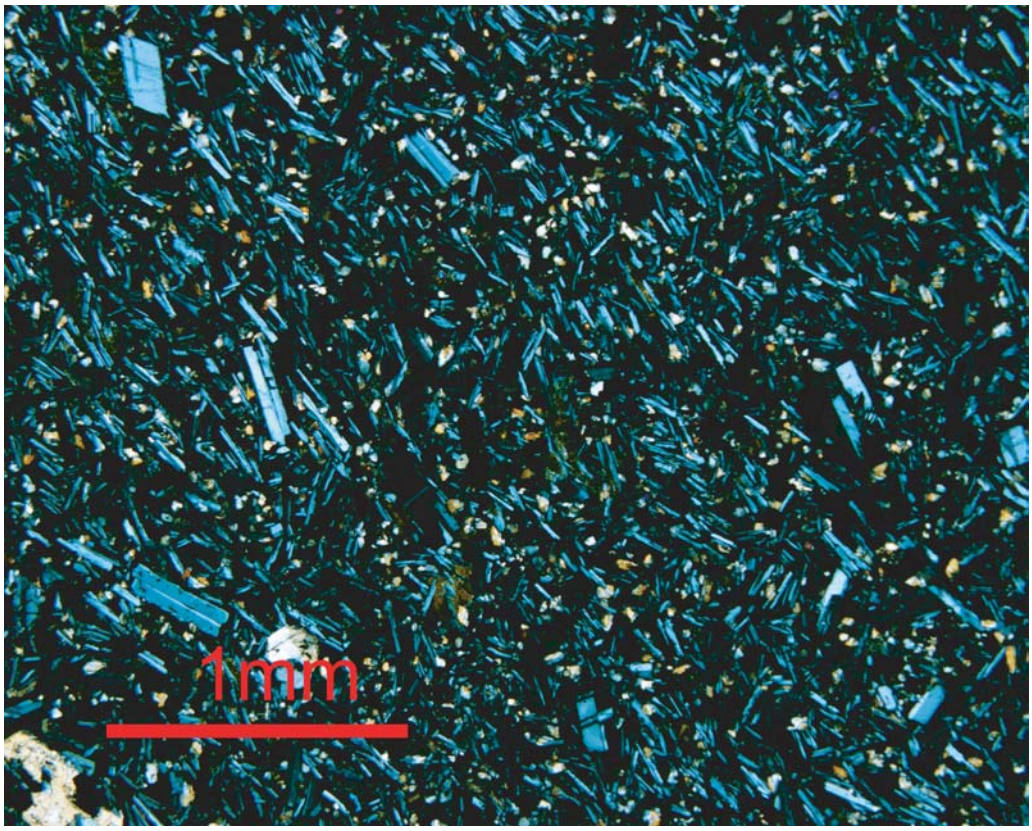

Figure 2: A photomicrograph of K-83-1694 showing euhedral to subhedral phenocrysts of plagioclase and pyroxene.

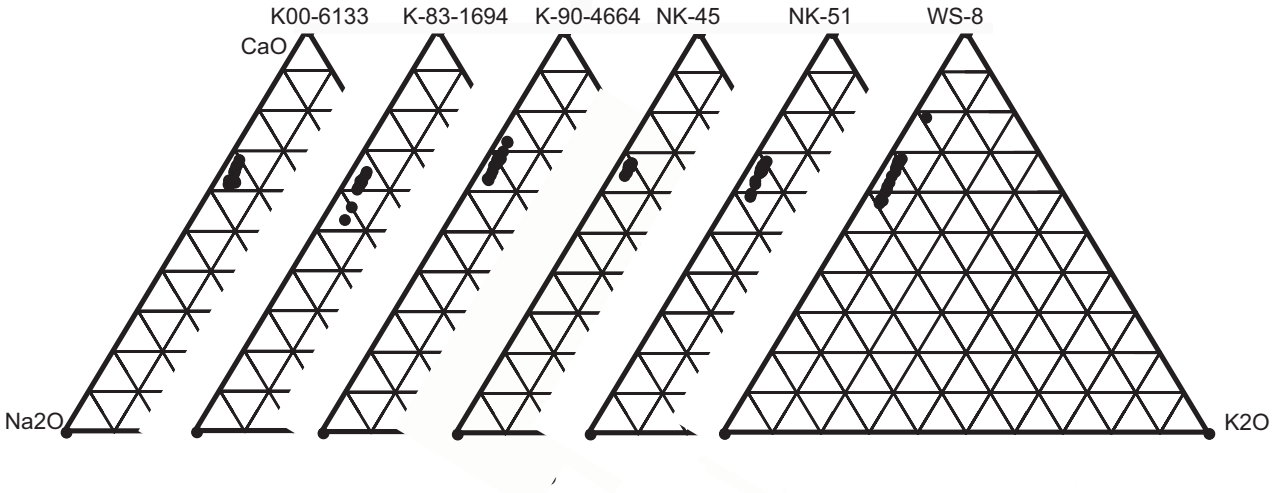

Figure 3: Plagioclase phenocryst compositions for each of the basalts. The compositional ranges of the plagioclase are similiar with almost all compositions plotting between An55 and An70. The phenocyrsts were weakly zoned; core compostions were more calcic rich and edge compositions were more sodic rich.

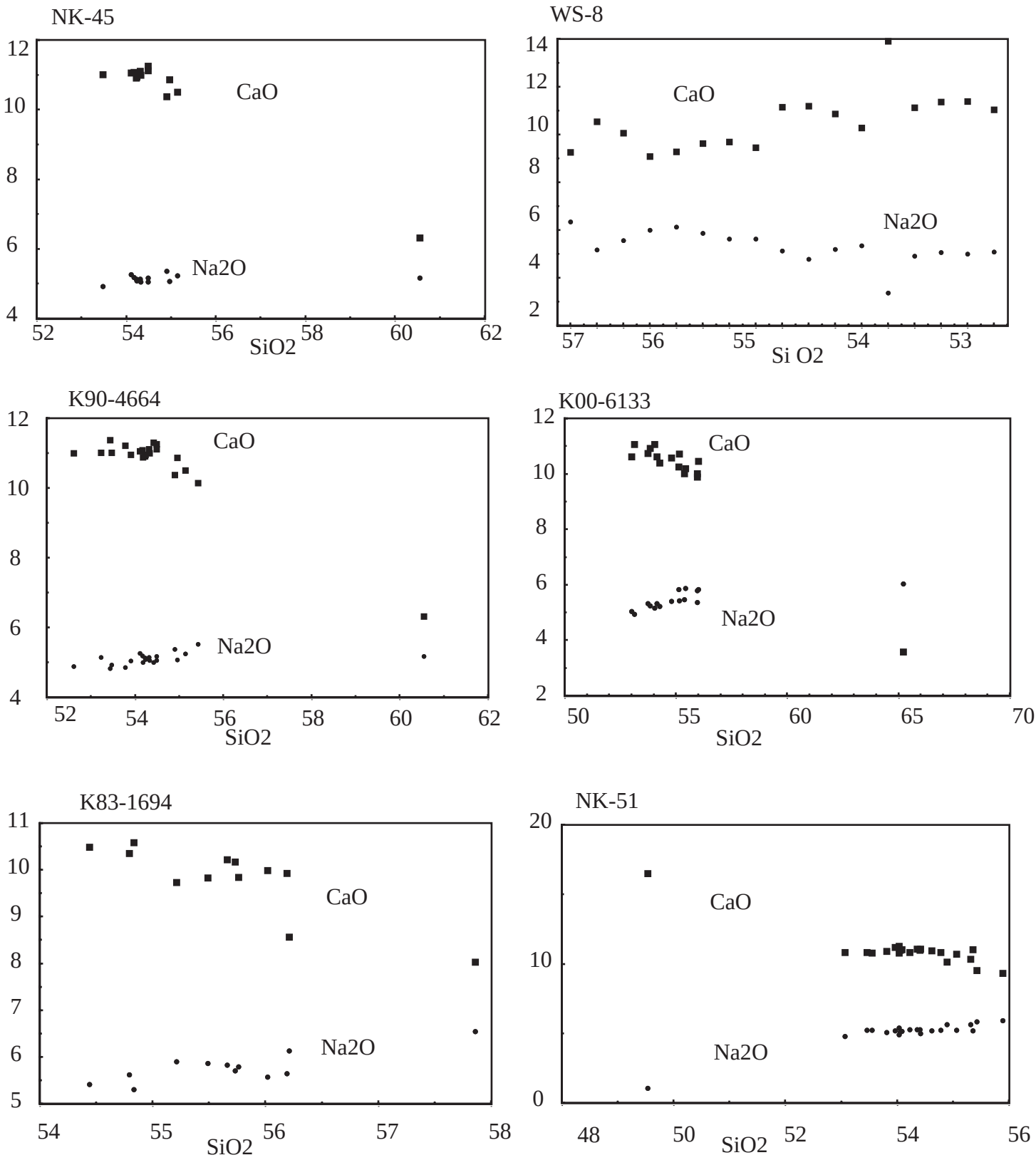

Figure 4. Variation diagrams of calcium and sodium oxides vs. silicon oxide show weak zoning in plagioclase phenocrysts with relatively more sodic cores and later crytalizing rims comparatively enriched in anothite.

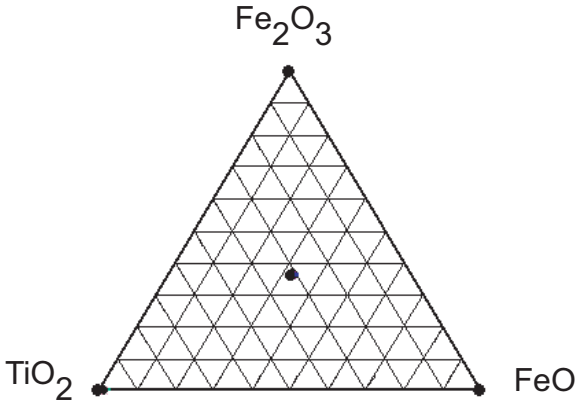

K-83-1694

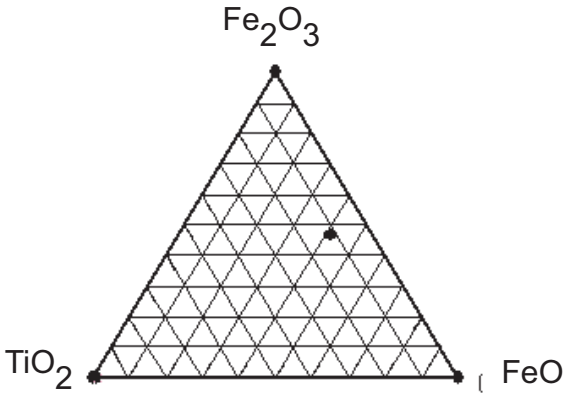

NK-45

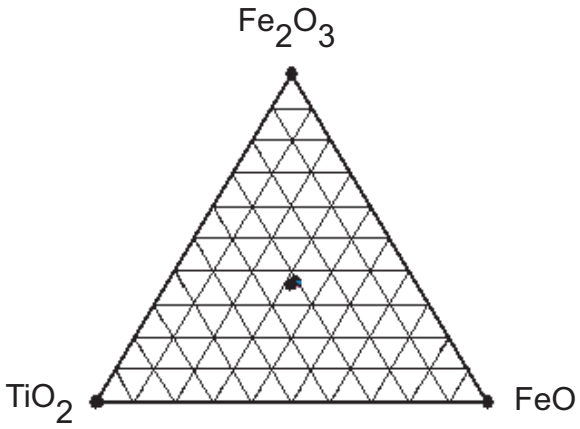

WS-8

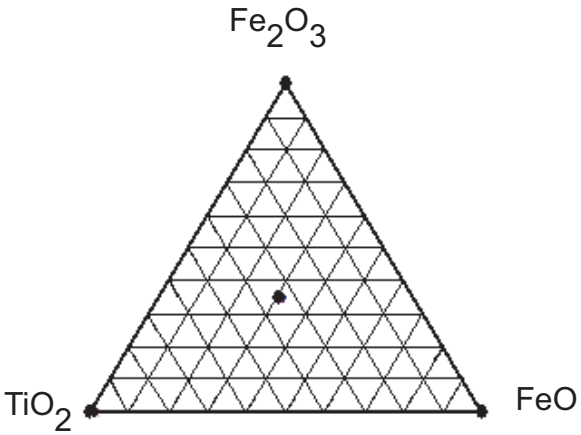

K-90-4664

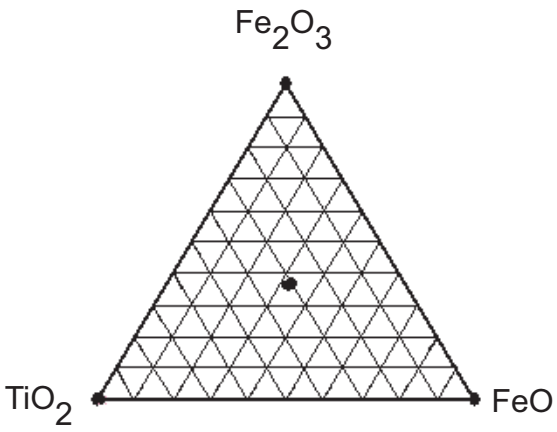

K-OO-6133

Figure 5: Ternary plot diagrams for ilmenite phenocryst compositions of basalt samples. Note the consistency of the chemical composition between the different samples. Points plot near the center of the diagrams, since normalized end-member values are about equal for each end member (each around 30-35%).

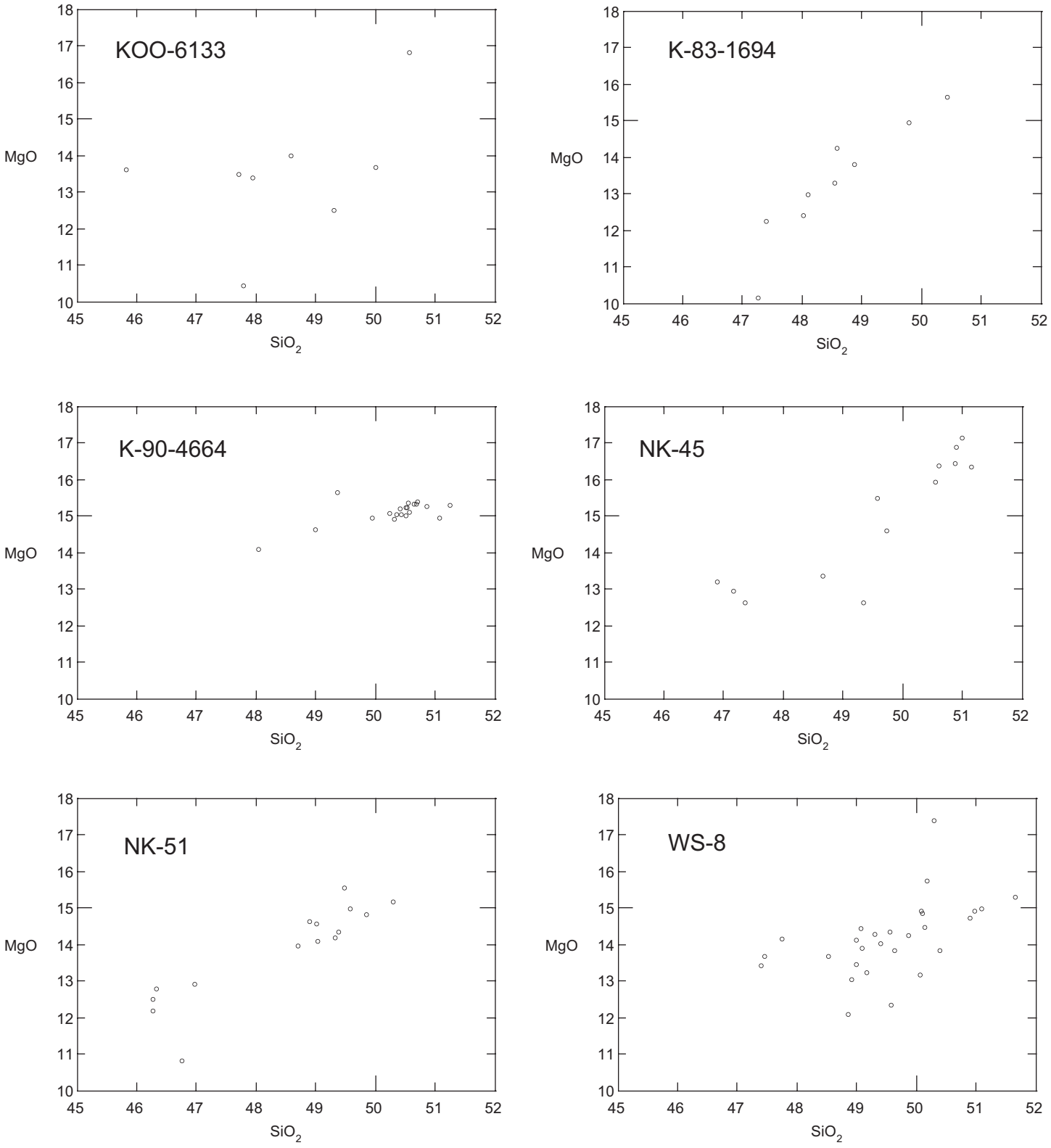

Figure 6: Harker variation diagrams of SiO2 vs. MgO for pyroxene phemocrysts for each of the basalts.

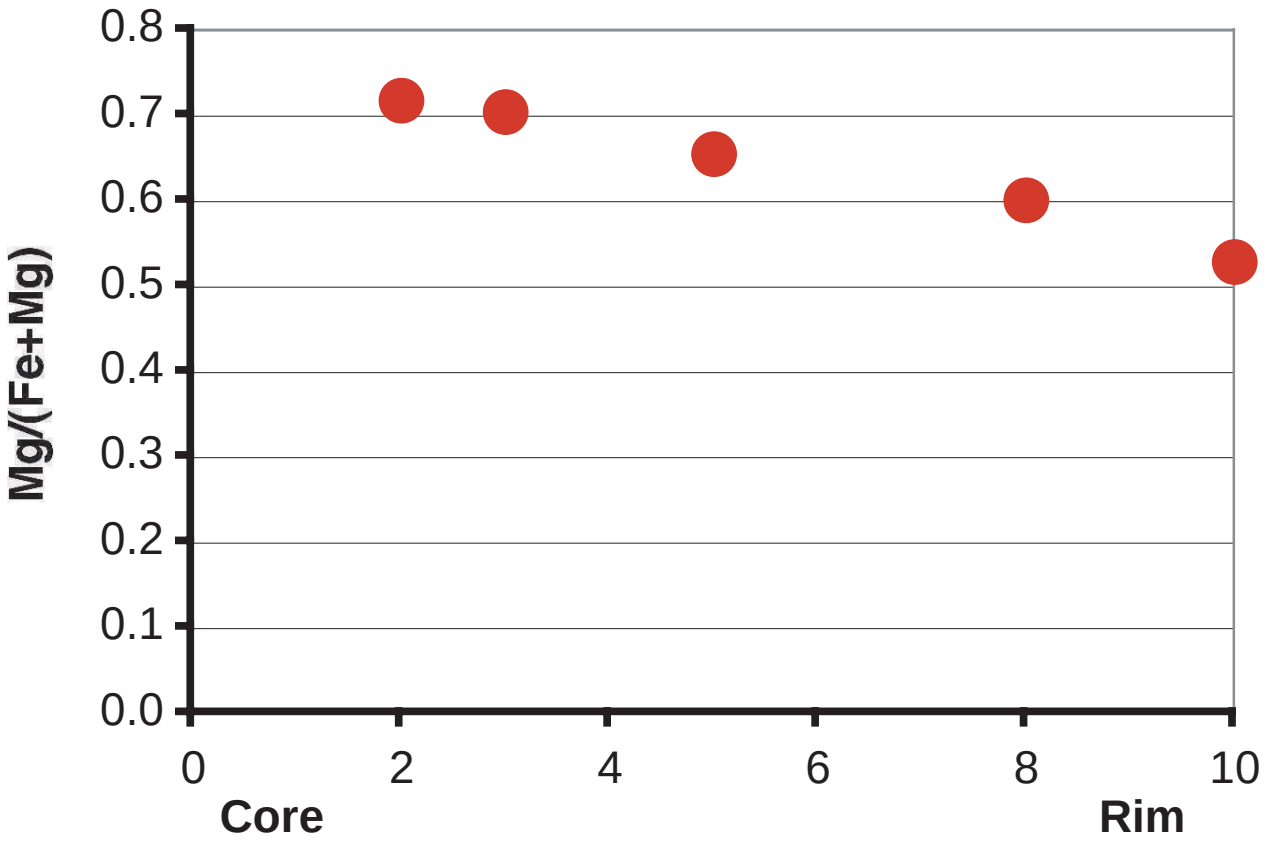

Figure 7. A plot of Mg/(Fe+Mg) values across a core to rim transect in a representative phenocryst demonstrates that pyroxene crystals show compositional zoning resulting in magnesium enriched cores and iron enriched rims.

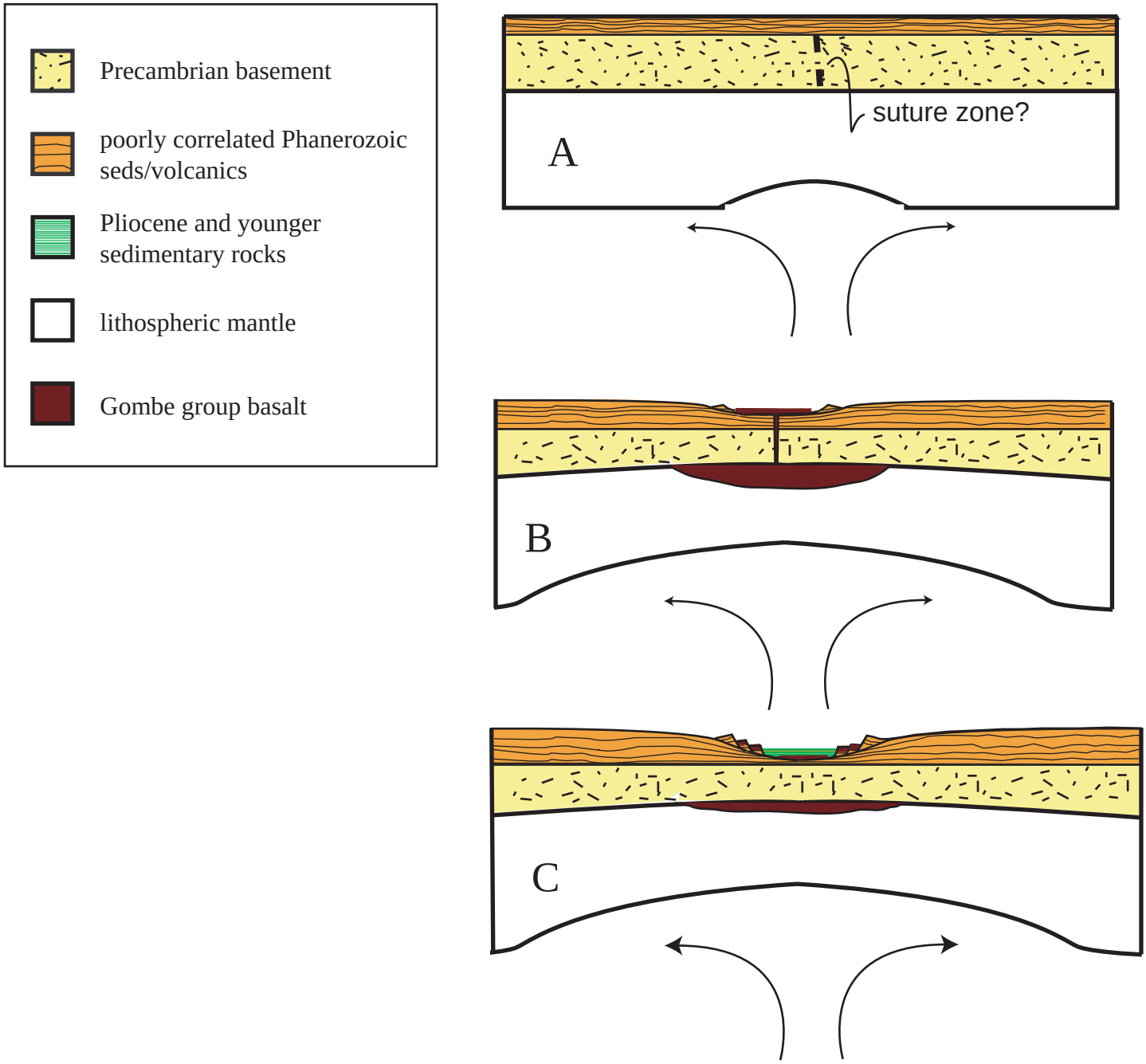

Figure 8: Our model for basin development: a) A convection cell thins the lithospheric mantle. b) Magma pools at the base of the crust and erupts to form Gombe Group basalts in the small basin that has formed. c) The basin continues to develop and fill with sediment.

Table 1: Plagioclase phenocryst chemistry for sample WS-8

WS-8	SiO2	TiO2	Na2O	Cr2O3	FeO	Al2O3	CaO	MgO	MnO	K2O
Core 1	57.57	0.09	6.35	0.06	0.85	27.69	9.25	0.08	0.02	0.52
Rim 1a	54.29	0.13	5.18	0.00	1.09	28.45	10.54	0.17	0.00	0.41
Rim 1b	55.05	0.12	5.57	0.00	1.13	27.78	10.06	0.12	0.00	0.43
Core 2	55.78	0.18	5.62	0.00	1.44	27.39	9.45	0.25	0.00	0.48
2a	55.26	0.16	5.62	0.02	0.78	27.23	9.69	0.10	0.03	0.43
2b	55.78	0.13	5.86	0.01	0.80	27.43	9.62	0.12	0.00	0.48
2c	56.28	0.18	6.13	0.00	0.89	27.23	9.29	0.12	0.00	0.47
Rim 2	57.00	0.38	6.00	0.00	1.00	27.36	9.09	0.10	0.00	0.55
Core 3	54.53	0.14	5.13	0.01	0.86	28.66	11.16	0.17	0.00	0.34
3a	54.12	0.12	4.78	0.00	1.01	28.43	11.19	0.11	0.00	0.37
3b	54.21	0.11	5.19	0.00	0.99	28.80	10.87	0.12	0.06	0.36
3c	55.25	0.15	5.35	0.01	1.08	27.92	10.28	0.17	0.01	0.37
Rim 3	54.61	0.57	3.36	0.07	6.17	17.13	13.92	6.13	0.15	0.38
Core 4	53.86	0.16	4.92	0.04	0.77	28.65	11.13	0.15	0.00	0.37
4a	54.18	0.07	5.06	0.00	0.82	29.05	11.36	0.14	0.00	0.31
4b	53.95	0.13	5.00	0.05	0.78	28.86	11.40	0.14	0.00	0.32
Rim 4	54.41	0.08	5.08	0.00	0.79	29.05	11.04	0.10	0.04	0.37

Table 2: Plagioclase phenocryst chemistry for sample NK-45

NK-45	SiO2	TiO2	Na2O	Cr2O3	FeO	Al2O3	CaO	MgO	MnO	K2O
Core 1	54.31	0.09	5.14	0.00	0.73	28.57	11.11	0.15	0.02	0.35
1a	54.11	0.11	5.26	0.00	0.73	28.36	11.06	0.14	0.02	0.34
1b	54.48	0.15	5.06	0.00	0.75	28.60	11.26	0.13	0.00	0.34
1c	55.14	0.10	5.24	0.02	0.76	28.04	10.51	0.14	0.02	0.38
Rim 1	60.55	0.26	5.17	0.00	2.07	20.33	6.32	0.13	0.04	2.10
Core 2	54.32	0.10	5.06	0.00	0.74	28.68	11.00	0.13	0.00	0.34
2a	54.23	0.19	5.08	0.06	0.96	28.52	10.95	0.17	0.01	0.40
2b	54.22	0.09	5.13	0.02	0.87	28.62	10.92	0.14	0.00	0.33
Rim 2	53.47	0.17	4.93	0.01	0.83	28.08	11.01	0.18	0.06	0.35
Core 3	54.96	0.22	5.07	0.00	0.82	28.38	10.87	0.13	0.00	0.33
3a	54.17	0.16	5.19	0.08	0.79	28.73	11.08	0.13	0.00	0.35
3b	54.48	0.12	5.17	0.03	0.95	28.60	11.12	0.16	0.00	0.30
Rim 3	54.90	0.17	5.37	0.04	1.06	27.96	10.37	0.16	0.00	0.36

Table 3: Plagioclase phenocryst chemistry for sample K83-1694

K-83	SiO2	TiO2	Na2O	Cr2O3	FeO	Al2O3	CaO	MgO	MnO	K2O
Core 1	57.86	0.11	6.54	0.00	0.88	25.89	8.03	0.10	0.00	0.62
1a	54.79	0.06	5.62	0.01	0.89	28.04	10.35	0.13	0.02	0.44
1b	54.44	0.14	5.41	0.00	0.98	27.93	10.49	0.15	0.02	0.45
Rim 1	55.49	0.20	5.87	0.00	0.97	27.44	9.83	0.16	0.04	0.44
Core 2	56.19	0.20	5.65	0.00	1.15	27.50	9.93	0.15	0.05	0.45
2a	54.83	0.14	5.30	0.00	0.94	28.22	10.59	0.15	0.01	0.42
Rim 2	56.21	0.17	6.13	0.05	0.96	26.34	8.57	0.13	0.00	0.60
Core 3	55.73	0.18	5.70	0.00	0.95	27.78	10.17	0.11	0.01	0.39
3a	55.66	0.16	5.83	0.00	0.98	27.75	10.22	0.12	0.00	0.45
3b	56.02	0.17	5.57	0.04	1.05	27.86	9.99	0.10	0.00	0.45
3c	55.76	0.21	5.79	0.00	1.22	27.71	9.84	0.15	0.04	0.45
Rim 3	55.21	0.18	5.90	0.00	1.22	27.46	9.73	0.09	0.00	0.45

Table 4: Plagioclase phenocryst chemistry for sample K90-4661

K-90	SiO2	TiO2	Na2O	Cr2O3	FeO	Al2O3	CaO	MgO	MnO	K2O
Core 1	54.03	0.09	5.12	0.00	0.84	28.69	10.85	0.16	0.04	0.30
1a	54.47	0.07	4.92	0.06	0.79	28.86	11.17	0.11	0.00	0.36
1b	54.02	0.14	4.99	0.03	0.83	28.74	11.37	0.14	0.00	0.39
1c	53.45	0.05	4.90	0.01	0.74	28.67	11.26	0.14	0.01	0.31
1d	53.69	0.11	4.95	0.00	0.77	29.10	11.24	0.09	0.04	0.29
1e	53.78	0.05	4.83	0.00	0.92	28.79	11.32	0.17	0.02	0.39
1f	52.49	0.16	4.39	0.00	0.77	29.50	12.32	0.14	0.03	0.30
1g	53.13	0.11	4.41	0.00	0.84	30.03	12.49	0.13	0.04	0.27
1h	53.96	0.12	4.77	0.00	0.81	28.87	11.43	0.13	0.02	0.31
Rim 1	53.47	0.14	4.68	0.03	0.85	28.98	11.82	0.13	0.04	0.34
Core 2	54.58	0.37	5.54	0.00	0.97	27.47	10.21	0.21	0.00	0.35
2a	54.28	0.16	5.34	0.00	1.05	27.83	10.76	0.21	0.03	0.37
2b	54.87	0.09	5.49	0.00	0.81	28.07	10.61	0.16	0.00	0.41
2c	55.43	0.12	5.52	0.00	0.83	27.65	10.14	0.08	0.00	0.41
2d	54.42	0.12	5.00	0.00	0.86	28.79	11.31	0.10	0.07	0.33
Rim 2	53.22	0.12	5.14	0.05	1.16	28.10	11.01	0.36	0.01	0.32
Core 3	53.90	0.07	5.04	0.00	0.92	28.34	10.96	0.13	0.00	0.36
3a	54.18	0.07	5.00	0.02	1.14	28.22	10.89	0.22	0.00	0.35
3b	53.77	0.14	4.85	0.03	0.95	28.67	11.22	0.13	0.01	0.31
3c	52.61	0.21	4.89	0.00	0.96	28.29	11.00	0.15	0.00	0.30
Rim 3	53.43	0.17	4.82	0.00	1.05	28.37	11.38	0.16	0.00	0.30

Table 5: Plagioclase phenocryst chemistry for sample K00-6133

K-00	SiO2	TiO2	Na2O	Cr2O3	FeO	Al2O3	CaO	MgO	MnO	K2O
Core 1	52.99	0.25	5.05	0.00	0.70	27.36	10.62	0.19	0.00	0.30
1a	54.04	0.09	5.17	0.03	0.70	28.55	11.07	0.11	0.00	0.32
1b	54.25	0.01	5.23	0.00	0.90	27.22	10.39	0.19	0.00	0.34
1c	54.78	0.08	5.40	0.00	0.73	28.01	10.57	0.13	0.00	0.39
1d	55.14	0.12	5.43	0.00	0.73	28.09	10.72	0.19	0.00	0.36
1e	53.74	0.09	5.33	0.01	0.79	28.18	10.74	0.12	0.04	0.35
1f	53.12	0.13	4.95	0.00	0.87	28.19	11.07	0.21	0.02	0.28
1g	53.83	0.10	5.25	0.02	0.76	28.19	10.93	0.15	0.00	0.32
Rim 1	54.13	0.12	5.32	0.04	0.83	28.47	10.63	0.21	0.00	0.34
Core 2	65.21	0.63	6.03	0.02	2.15	18.08	3.58	0.08	0.00	2.10
2a	55.95	0.14	5.37	0.04	0.89	27.41	9.89	0.15	0.00	0.55
Rim 2	55.11	0.13	5.83	0.02	0.80	27.92	10.26	0.11	0.00	0.41
Core 3	55.96	0.19	5.79	0.03	0.89	27.46	10.02	0.13	0.00	0.46
Rim 3	55.36	0.23	5.47	0.00	0.91	27.17	10.02	0.16	0.03	0.60
Core 4	55.41	0.26	5.87	0.00	0.95	27.39	10.19	0.17	0.02	0.42
Rim 4	56.00	0.09	5.83	0.00	0.93	28.07	10.45	0.11	0.00	0.35

Table 6: Plagioclase phenocryst chemistry for sample NK-51

NK-51	SiO2	TiO2	Na2O	Cr2O3	FeO	Al2O3	CaO	MgO	MnO	K2O
Core 1	55.31	0.18	5.62	0.00	1.09	27.51	10.34	0.18	0.00	0.39
1a	54.05	0.12	5.13	0.00	0.80	28.40	11.01	0.14	0.02	0.38
1b	54.62	0.15	5.18	0.00	0.93	28.61	10.94	0.14	0.00	0.39
Rim 1	54.78	0.12	5.25	0.04	0.83	28.47	10.84	0.11	0.02	0.34
Core 2	55.06	0.24	5.23	0.01	0.93	28.02	10.70	0.19	0.00	0.42
2a	55.35	0.30	5.20	0.00	1.47	27.12	11.04	0.59	0.04	0.39
2b	54.41	0.13	5.28	0.04	1.05	28.11	11.01	0.24	0.04	0.44
2c	54.42	0.12	5.01	0.01	0.90	28.61	11.06	0.15	0.00	0.38
2d	54.03	0.10	4.92	0.08	0.94	28.38	11.27	0.20	0.02	0.38
2e	54.36	0.21	5.27	0.00	0.99	28.69	11.06	0.20	0.02	0.37
2f	54.08	0.09	5.17	0.02	0.81	28.55	11.03	0.11	0.02	0.34
2g	54.03	0.18	5.39	0.00	0.97	27.86	10.79	0.12	0.00	0.39
2h	54.89	0.22	5.65	0.04	1.02	27.32	10.14	0.12	0.05	0.46
Rim 2	55.89	0.24	5.92	0.02	0.98	26.92	9.35	0.19	0.00	0.53
Core 3	53.96	0.13	5.18	0.00	0.82	28.51	11.21	0.17	0.01	0.34
3a	53.06	0.11	4.79	0.04	0.89	27.93	10.82	0.18	0.00	0.34
3b	53.81	0.10	5.09	0.02	1.14	27.59	10.90	0.24	0.00	0.38
Rim 3	55.43	0.10	5.85	0.01	1.13	27.03	9.54	0.18	0.00	0.51
Core 4	54.22	0.14	5.28	0.00	0.93	28.24	10.85	0.13	0.02	0.36
4a	53.46	0.17	5.23	0.00	0.89	27.51	10.82	0.18	0.01	0.34
Rim 4	53.55	0.14	5.24	0.00	1.29	27.46	10.80	0.30	0.03	0.37

Table 7: Ilmenite phenocryst chemistry for all samples.

WS-8	SiO_2	TiO_2	Na_2O	Fe_2O_3	Cr_2O_3	FeO	Al_2O3	CaO	MgO	MnO	K_2O
Core 1	0.22	45.51	0.03	52.14	0.07	46.97	0.27	0.15	0.87	0.58	0.05
Rim 1a	0.26	43.85	0.08	52.18	0.04	47.01	0.47	0.10	1.12	0.53	0.04
Rim 1b	0.26	45.02	0.04	52.99	0.03	47.74	0.23	0.08	0.85	0.54	0.01
Core 2	0.05	47.54	0.00	52.75	0.02	47.53	0.19	0.06	1.22	0.53	0.01
2b	0.09	46.94	0.06	52.18	0.00	47.01	0.26	0.05	1.58	0.53	0.02
2c	0.12	46.61	0.03	52.09	0.00	46.93	0.25	0.04	1.35	0.52	0.03
Rim2	0.13	46.90	0.00	53.26	0.00	47.98	0.21	0.08	1.60	0.49	0.03
Core 3	0.07	47.94	0.01	52.14	0.04	46.97	0.21	0.05	1.22	0.57	0.03
3b	0.09	46.55	0.04	52.36	0.02	47.17	0.24	0.03	1.42	0.51	0.05
3c	0.04	47.12	0.00	53.08	0.00	47.82	0.27	0.06	1.53	0.45	0.02
3d	0.09	46.78	0.07	52.98	0.08	47.73	0.19	0.07	1.40	0.61	0.00
3e	0.12	46.72	0.05	53.19	0.06	47.92	0.20	0.07	1.60	0.53	0.01
3f	0.21	45.99	0.06	52.58	0.07	47.37	0.27	0.10	1.54	0.50	0.03
3g	0.14	46.68	0.06	53.09	0.00	47.83	0.27	0.09	1.35	0.64	0.02
3 Rim	0.53	45.92	0.20	52.67	0.00	47.45	0.29	0.16	1.38	0.59	0.02
Core 4	0.14	46.45	0.02	52.76	0.00	47.53	0.19	0.20	1.50	0.56	0.08
Rim 4	67.37	1.08	2.72	2.13	0.00	1.92	13.49	2.34	0.08	0.07	2.17
NK-45											
	21.62	13.47	2.29	54.71	0.04	49.29	8.29	1.97	0.71	0.39	0.73
K83-1694											
Core 1	0.03	47.41	0.00	54.68	0.00	49.26	0.39	0.08	1.63	0.49	0.04
1b	0.10	47.43	0.04	54.70	0.00	49.28	0.42	0.08	1.77	0.41	0.03
1c	0.04	47.82	0.04	54.95	0.00	49.50	0.32	0.08	1.72	0.51	0.05
1d	0.05	47.71	0.02	55.00	0.00	49.55	0.36	0.14	1.75	0.50	0.02
Rim 1	0.06	47.53	0.06	54.90	0.09	49.46	0.38	0.11	1.76	0.48	0.04
Core 2	0.05	47.32	0.01	54.67	0.00	49.25	0.35	0.08	1.84	0.43	0.00
2b	0.10	47.45	0.04	53.97	0.00	48.63	0.41	0.16	1.81	0.45	0.01
Rim 2	0.52	47.24	0.06	53.20	0.00	47.93	0.45	0.26	2.00	0.47	0.07
K90-4661											
Core 1	0.11	50.52	0.06	51.46	0.02	46.36	0.34	0.06	2.81	0.55	0.00
1b	0.07	50.47	0.06	51.30	0.00	46.22	0.26	0.02	2.78	0.56	0.03
1c	0.07	50.51	0.05	51.80	0.04	46.67	0.32	0.04	2.94	0.56	0.04
1d	0.89	49.12	0.09	50.26	0.00	45.28	0.64	0.10	2.70	0.52	0.04
1e	0.37	50.05	0.01	51.42	0.02	46.33	0.34	0.07	2.96	0.53	0.03
1f	0.06	50.01	0.06	52.28	0.00	47.10	0.27	0.00	2.86	0.51	0.04
1g	0.04	50.50	0.00	51.82	0.06	46.69	0.31	0.03	2.78	0.59	0.03
1h	0.33	49.98	0.15	51.16	0.00	46.09	0.38	0.08	2.88	0.53	0.03
Rim 1	0.05	49.85	0.00	51.91	0.00	46.77	0.28	0.06	2.82	0.56	0.03
Core 2	0.21	47.40	0.22	52.76	0.00	47.53	0.26	0.17	1.23	0.55	0.08
K00-6133											
Core 1	0.41	44.48	0.00	54.39	0.07	49.00	0.45	0.23	1.45	0.42	0.02
Rim 1	0.06	46.90	0.00	55.65	0.00	50.14	0.35	0.11	1.55	0.38	0.07

Table 8: Pyroxene phenocryst chemistry for sample WS-8

WS-8	SiO2	TiO2	Na2O	Cr2O3	FeO	Al2O3	CaO	MgO	MnO	K2O
1	50.29	0.43	0.96	0.97	4.77	8.03	16.99	17.37	0.15	0
2	16.48	1.7	0.4	0.09	10.24	1.38	14.59	9.63	0.24	0.02
3	50.9	1.11	0.38	0.09	10.29	2.04	19.31	14.73	0.21	0.03
4	50.08	1.33	0.4	0.08	11.13	2.3	18.69	14.9	0.29	0.02
5	47.41	1.36	0.31	0.05	11.63	2.28	18.63	13.41	0.3	0.04
6	49.1	1.54	0.37	0.06	13.02	2.4	17.61	13.9	0.34	0.01
7	49	1.44	0.38	0.02	13.52	2.49	17.41	14.12	0.32	0.04
8	16.45	1.05	0.33	0.01	12.61	0.9	13.84	10.03	0.25	0.01
9	50.4	0.83	0.29	0	16.29	1.42	15.4	13.81	0.39	0.04
10	49.17	0.72	0.27	0	17.33	1.32	15.1	13.21	0.42	0.03
11	49.58	0.58	0.27	0	19.54	1.43	14.77	12.33	0.49	0.06
12	50.97	1.01	0.29	0	11.16	1.74	18.94	14.9	0.26	0.03
13	51.66	1.11	0.34	0.03	10.73	1.85	19.17	15.29	0.23	0.03
14	50.18	1.16	0.34	0.11	10.73	1.94	18.88	15.72	0.29	0.04
15	51.09	1.12	0.36	0.09	10.84	1.88	18.95	14.97	0.29	0.03
16	50.14	1.24	0.45	0.09	11.59	1.91	18.31	14.47	0.24	0.01
17	49.88	1.42	0.43	0.05	12.62	2.58	17.92	14.25	0.28	0.03
18	48.99	1.36	0.4	0.01	13.88	2.63	17.19	13.44	0.33	0.04
19	49.64	1.17	0.41	0.01	14.23	2.31	17.41	13.83	0.37	0.05
20	50.06	1.12	0.33	0.01	14.83	2.06	17.65	13.16	0.33	0.04
21	48.86	0.88	0.39	0	17.08	1.95	16.83	12.07	0.33	0.06
22	47.45	2.32	0.51	0.04	12.14	4.06	18.24	13.67	0.27	0.06
23	48.52	1.83	0.52	0.07	11.47	3.64	17.77	13.67	0.24	0.1
24	49.08	1.47	0.41	0.16	10.89	2.48	18.99	14.42	0.29	0.02
25	47.76	1.07	0.32	0.09	10.85	2.07	18.04	14.15	0.22	0.03
26	50.11	1.24	0.37	0.1	11.38	2.2	18.49	14.83	0.31	0.01
27	49.56	1.39	0.42	0	11.98	2.35	18.21	14.34	0.27	0.02
28	49.3	1.58	0.4	0.02	12.79	2.46	17.36	14.26	0.26	0.02
29	49.41	1.43	0.51	0.01	13.43	2.3	16.78	14.02	0.29	0.01
30	48.91	1.11	0.6	0.03	13.76	2.69	16.74	13.02	0.32	0.03
31	53.64	0.25	5.02	0	3.2	22.72	10.18	2.09	0.1	0.43

Table 9: Pyroxene phenocryst chemistry for sample NK-45

NK-45	SiO2	TiO2	Na2O	Cr2O3	FeO	Al2O3	CaO	MgO	MnO	K2O
47	50.90	0.93	0.19	0.04	14.19	1.31	14.06	16.86	0.36	0.04
48	50.89	0.91	0.27	0.00	14.21	1.38	14.81	16.44	0.36	0.03
49	50.55	1.02	0.27	0.02	14.07	1.64	15.47	15.93	0.41	0.03
50	49.74	1.43	0.34	0.01	13.44	2.54	16.55	14.59	0.36	0.04
51	49.35	1.66	0.62	0.13	12.31	3.80	17.30	12.63	0.29	0.33
52	50.61	1.10	0.20	0.00	15.48	1.57	14.06	16.37	0.43	0.01
53	46.89	2.49	0.45	0.04	14.00	3.91	17.12	13.20	0.29	0.04
54	47.16	2.58	0.42	0.04	14.35	3.93	17.43	12.94	0.35	0.01
55	1.33	0.00	0.02	0.02	1.21	0.09	51.28	0.34	0.59	0.03
56	0.00	0.00	0.00	0.00	0.88	0.01	56.71	0.37	0.90	0.00
57	0.00	0.03	0.05	0.02	0.67	0.01	57.02	0.35	0.76	0.01
58	6.23	0.00	0.09	0.04	3.22	0.46	45.75	0.51	0.70	0.04
59	9.45	0.05	0.11	0.02	4.33	0.70	43.76	0.59	0.60	0.03
60	16.24	0.07	0.12	0.03	6.91	1.22	37.96	0.92	0.61	0.04
61	23.62	0.10	0.14	0.00	8.03	2.38	18.65	1.49	0.31	0.16
62	40.47	0.17	0.45	0.00	12.27	4.70	2.35	2.72	0.09	0.16
63	36.09	0.15	0.20	0.00	10.66	4.24	2.19	2.67	0.09	0.19
64	41.46	0.18	0.49	0.00	12.92	4.85	2.20	2.44	0.10	0.26
65	51.00	1.04	0.26	0.00	14.74	1.39	13.68	17.14	0.39	0.00
66	49.57	1.23	0.23	0.00	14.41	2.00	14.89	15.49	0.40	0.04
67	51.16	1.20	0.23	0.00	15.36	1.71	14.01	16.32	0.33	0.03
68	48.66	2.22	0.36	0.00	14.58	3.08	17.53	13.34	0.34	0.00
69	47.36	2.38	0.28	0.04	15.92	2.81	16.78	12.62	0.36	0.01

Table 10: Pyroxene phenocryst chemistry for sample K83-1694

K-83	SiO2	TiO2	Na2O	Cr2O3	FeO	Al2O3	CaO	MgO	MnO	K2O
100	48.11	1.58	0.38	0.04	16.54	3.01	16.30	12.98	0.41	0.03
101	48.02	1.44	0.33	0.01	17.31	2.28	16.16	12.39	0.47	0.04
102	47.26	1.10	0.39	0.00	21.39	1.83	15.41	10.15	0.52	0.05
103	47.40	1.50	0.34	0.00	17.67	2.65	15.84	12.25	0.39	0.04
104	48.55	1.55	0.36	0.00	17.02	2.88	15.32	13.29	0.41	0.00
105	48.87	1.70	0.35	0.06	15.85	3.14	15.50	13.78	0.39	0.02
106	37.52	12.63	0.18	0.00	24.77	1.05	7.72	13.22	0.40	0.08
107	0.05	47.32	0.01	0.00	49.25	0.35	0.08	1.84	0.43	0.00
108	0.10	47.45	0.04	0.00	48.63	0.41	0.16	1.81	0.45	0.01
109	0.52	47.24	0.06	0.00	47.93	0.45	0.26	2.00	0.47	0.07
110	29.91	13.81	4.48	0.04	33.15	9.72	2.34	1.60	0.21	1.92
111	17.11	0.22	0.41	0.01	39.83	1.82	3.25	7.29	1.02	0.37
112	31.79	0.81	0.32	0.03	28.73	2.15	10.48	11.20	0.53	0.12
113	48.59	1.18	0.34	0.01	12.98	2.25	16.99	14.23	0.31	0.07
114	50.43	1.38	0.30	0.00	12.91	2.26	16.92	15.64	0.28	0.03
115	49.80	1.31	0.31	0.03	13.60	2.15	16.50	14.93	0.38	0.02
116	0.03	47.41	0.00	0.00	49.26	0.39	0.08	1.63	0.49	0.04
117	0.10	47.43	0.04	0.00	49.28	0.42	0.08	1.77	0.41	0.03
118	0.04	47.82	0.04	0.00	49.50	0.32	0.08	1.72	0.51	0.05
119	0.05	47.71	0.02	0.00	49.55	0.36	0.14	1.75	0.50	0.02
120	0.06	47.53	0.06	0.09	49.46	0.38	0.11	1.76	0.48	0.04

Table 11: Pyroxene phenocryst chemistry for sample K90-4661

K-90	SiO2	TiO2	Na2O	Cr2O3	FeO	Al2O3	CaO	MgO	MnO	K2O
70	49.00	0.99	0.35	0.05	13.26	2.47	15.89	14.62	0.28	0.11
71	50.24	1.06	0.37	0.00	11.43	2.11	18.00	15.05	0.29	0.05
72	51.08	1.06	0.26	0.06	11.63	1.86	18.47	14.94	0.32	0.02
73	48.05	1.20	0.41	0.03	11.43	1.82	17.93	14.09	0.35	0.02
74	50.52	1.03	0.34	0.00	11.48	1.79	18.30	15.22	0.31	0.04
75	50.87	1.01	0.30	0.02	12.15	1.61	18.13	15.25	0.36	0.04
76	49.94	1.00	0.30	0.06	12.28	1.75	17.77	14.93	0.32	0.06
77	50.55	1.00	0.36	0.01	12.60	1.63	17.44	15.35	0.38	0.05
78	50.35	1.05	0.32	0.01	12.90	1.80	17.36	15.02	0.37	0.02
79	51.26	0.93	0.28	0.00	12.50	1.61	17.52	15.29	0.32	0.03
80	0.11	50.52	0.06	0.02	46.36	0.34	0.06	2.81	0.55	0.00
81	0.07	50.47	0.06	0.00	46.22	0.26	0.02	2.78	0.56	0.03
82	0.07	50.51	0.05	0.04	46.67	0.32	0.04	2.94	0.56	0.04
83	0.89	49.12	0.09	0.00	45.28	0.64	0.10	2.70	0.52	0.04
84	0.37	50.05	0.01	0.02	46.33	0.34	0.07	2.96	0.53	0.03
85	0.06	50.01	0.06	0.00	47.10	0.27	0.00	2.86	0.51	0.04
86	0.04	50.50	0.00	0.06	46.69	0.31	0.03	2.78	0.59	0.03
87	0.33	49.98	0.15	0.00	46.09	0.38	0.08	2.88	0.53	0.03
88	0.05	50.93	0.04	0.00	46.38	0.28	0.02	2.87	0.49	0.03
89	0.05	49.85	0.00	0.00	46.77	0.28	0.06	2.82	0.56	0.03
90	50.43	1.00	0.38	0.00	11.85	1.98	17.80	15.04	0.31	0.06
91	50.32	1.24	0.35	0.00	11.22	1.98	18.57	14.90	0.33	0.05
92	50.53	1.14	0.39	0.00	11.65	2.09	18.59	15.21	0.30	0.02
93	50.52	1.20	0.35	0.00	11.40	1.99	18.93	15.01	0.33	0.01
94	50.71	0.95	0.28	0.00	11.41	1.75	18.52	15.37	0.27	0.03
95	50.69	1.01	0.28	0.00	11.41	1.79	18.46	15.31	0.32	0.04
96	50.65	1.05	0.34	0.03	11.40	1.77	18.26	15.31	0.32	0.03
97	50.41	1.07	0.28	0.06	11.40	1.85	18.63	15.20	0.31	0.03
98	50.58	1.07	0.30	0.00	11.52	1.95	18.30	15.10	0.24	0.02
99	49.36	1.26	0.44	0.03	11.71	2.13	18.31	15.64	0.31	0.05

Table 12: Pyroxene phenocryst chemistry for sample K00-6133

K-00	SiO2	TiO2	Na2O	Cr2O3	FeO	Al2O3	CaO	MgO	MnO	K2O
121	0.41	44.48	0.00	0.07	49.00	0.45	0.23	1.45	0.42	0.02
122	0.06	46.90	0.00	0.00	50.14	0.35	0.11	1.55	0.38	0.07
123	49.30	1.17	0.30	0.00	20.99	1.63	12.76	12.49	0.49	0.11
124	47.94	1.17	0.22	0.00	20.18	1.68	12.09	13.38	0.57	0.07
125	47.71	2.08	0.29	0.00	15.38	3.23	16.38	13.48	0.36	0.00
126	50.00	1.04	0.22	0.00	19.75	1.59	12.85	13.67	0.52	0.04
127	47.79	1.64	0.30	0.01	20.76	2.35	15.94	10.43	0.52	0.04
128	50.57	0.96	0.25	0.03	15.37	1.57	12.80	16.82	0.40	0.04
129	45.83	1.53	0.27	0.00	14.37	2.52	15.36	13.59	0.38	0.03
130	48.58	1.70	0.36	0.00	15.38	3.08	15.87	13.99	0.38	0.03
131	41.61	8.19	0.33	0.06	21.78	2.35	13.09	12.38	0.45	0.02

Table 13: Pyroxene phenocryst chemistry for sample NK-51

NK-51	SiO2	TiO2	Na2O	Cr2O3	FeO	Al2O3	CaO	MgO	MnO	K2O
32	49.03	1.69	0.38	0.07	12.13	2.97	18.59	14.07	0.26	0.02
33	49.32	1.75	0.35	0.06	12.50	2.91	18.18	14.18	0.26	0.05
34	49.86	1.60	0.35	0.09	12.98	2.64	17.15	14.82	0.29	0.02
35	46.28	1.26	0.35	0.00	16.35	2.85	15.27	12.16	0.35	0.09
36	48.90	1.48	0.35	0.02	12.15	2.63	17.32	14.62	0.23	0.03
37	49.39	1.60	0.38	0.03	12.17	2.86	18.68	14.33	0.29	0.01
38	50.30	1.24	0.32	0.10	12.35	2.18	17.14	15.17	0.26	0.04
39	48.70	1.59	0.43	0.13	12.78	2.89	17.36	13.96	0.32	0.05
40	46.34	2.21	0.35	0.06	13.72	3.14	17.36	12.78	0.33	0.02
41	46.76	1.75	0.38	0.03	18.37	3.22	15.99	10.82	0.40	0.06
42	49.02	1.67	0.34	0.07	11.95	2.84	18.21	14.54	0.27	0.03
43	49.58	1.43	0.29	0.10	12.11	2.39	17.79	14.97	0.29	0.02
44	49.49	1.52	0.29	0.08	12.95	2.20	16.86	15.54	0.28	0.00
45	46.97	2.11	0.52	0.04	13.36	3.29	17.07	12.90	0.27	0.03
46	46.27	2.98	0.48	0.00	15.31	4.32	17.30	12.48	0.30	0.03

Table 14: Representative pyroxene chemistry for core and rim

	WS-8		KOO-6133		NK-51		K90-4661		K83-1694	
	Core	**Rim**	**Core**	**Rim**	**Core**	**Rim**	**Core**	**Rim**	**Core**	**Rim**
SiO2	50.90	49.28	50.57	47.79	49.02	46.51	50.43	50.31	48.11	47.26
Al2O3	2.04	1.89	1.57	2.35	2.84	3.77	1.98	1.87	3.01	1.83
TiO2	1.11	0.96	0.96	1.64	1.67	2.37	1.00	1.09	1.58	1.10
Cr2O3	0.09	0.00	0.03	0.01	0.07	0.01	0.00	0.01	0.04	0.00
FeO	10.29	16.28	15.37	20.76	11.95	16.84	11.85	12.10	16.54	21.39
MgO	14.73	12.81	16.82	10.43	14.54	11.65	15.04	15.47	12.98	10.15
MnO	0.21	0.37	0.40	0.52	0.27	0.35	0.31	0.32	0.41	0.52
CaO	19.31	16.13	12.80	15.94	18.21	16.65	17.80	17.92	16.30	15.41
K2O	0.03	0.04	0.04	0.04	0.03	0.04	0.06	0.04	0.03	0.05
Na2O	0.38	0.39	0.25	0.30	0.34	0.43	0.38	0.36	0.38	0.39
total:	99.08	98.55	98.80	99.78	98.94	98.63	98.84	99.49	99.38	98.10
Cations based on 6 Oxygens										
Si	1.92	1.92	1.92	1.87	1.87	1.82	1.92	1.90	1.86	1.89
Al(iv)	0.08	0.08	0.08	0.13	0.13	0.18	0.08	0.10	0.14	0.11
Al(vi)	0.01	0.01	0.00	0.00	0.00	0.00	0.00	0.00	0.00	0.00
Ti	0.03	0.03	0.03	0.05	0.05	0.07	0.03	0.03	0.05	0.03
Cr	0.00	0.00	0.00	0.00	0.00	0.00	0.00	0.00	0.00	0.00
Fe	0.32	0.53	0.49	0.68	0.38	0.55	0.38	0.38	0.53	0.72
Mg	0.83	0.74	0.95	0.61	0.83	0.68	0.85	0.87	0.75	0.61
Mn	0.01	0.01	0.01	0.02	0.01	0.01	0.01	0.01	0.01	0.02
Ca	0.78	0.67	0.52	0.67	0.74	0.70	0.72	0.73	0.67	0.66
K	0.00	0.00	0.00	0.00	0.00	0.00	0.00	0.00	0.00	0.00
Na	0.03	0.03	0.02	0.02	0.03	0.03	0.03	0.03	0.03	0.03
total:	4.02	4.02	4.02	4.04	4.03	4.04	4.03	4.04	4.04	4.05
Mg/(Fe+Mg):	0.718	0.584	0.661	0.472	0.684	0.552	0.693	0.695	0.583	0.458